

## First-Principles Study of Aqueous Hydroxide Solutions

Bin Chen,<sup>\*,†</sup> Jung Mee Park,<sup>‡,§</sup> Ivaylo Ivanov,<sup>†</sup> Gloria Tabacchi,<sup>‡,#</sup> Michael L. Klein,<sup>†</sup> and Michele Parrinello<sup>‡,⊥,||</sup>

Center for Molecular Modeling and Department of Chemistry, University of Pennsylvania, 231 South 34th Street, Philadelphia, Pennsylvania 19104-6323, Max-Planck-Institut für Festkörperforschung, Heisenbergstrasse 1, 70569 Stuttgart, Germany, Department of Chemistry, Division of Molecular and Life Sciences, Pohang University of Science and Technology, San 31, Hyojadong, Nambu, Pohang 790-784, Korea, Centro Svizzero di Calcolo Scientifico (CSCS), via Cantonale, 6928 Manno, Switzerland, Physical Chemistry, ETH Zurich, Hönggerberg, 8093 Zurich, Switzerland

Received March 7, 2002

The structural and dynamical properties of water change significantly in the presence of hydroxide ions ( $\text{OH}^-$ ). For example, data from a recent neutron diffraction with isotopic substitution (NDIS) experiment suggest that the characteristic tetrahedral short-range coordination of water is totally absent in a 40 wt % NaOH solution.<sup>1</sup> Also, new spectroscopic features appear which are quite distinct from those of pure water.<sup>2</sup> Despite many experiments, confusion persists regarding the solvation structures of  $\text{OH}^-$ .<sup>3</sup> Spectroscopic experiments on concentrated solutions<sup>2</sup> suggest that  $\text{H}_3\text{O}_2^-$  is the dominant solvation structure, whereas gas-phase mass spectrometric measurements and gas-phase ab initio calculations point to a shell closure at three water molecules.<sup>4</sup> However, these findings are seemingly at odds with Car–Parrinello molecular dynamics (CPMD) simulations,<sup>5</sup> which identified  $\text{H}_3\text{O}_5^-$  as the dominant structure, with four waters hydrogen bonded to  $\text{OH}^-$  in a roughly planar conformation.<sup>6</sup>

In this Communication, we report new structural and dynamical information on aqueous hydroxides obtained from CPMD simulations<sup>7</sup> on five NaOH/ $\text{H}_2\text{O}$  systems [(i) 0/64 (0 M), (ii) 1/36 (1.5 M), (iii) 3/36 (4.5 M), (iv) 8/24 (15 M), and (v) 16/48 (15 M)] and two KOH/ $\text{H}_2\text{O}$  systems [(vi) 1/43 (1.3 M) and (vii) 11/32 (14 M)]. For the most concentrated NaOH solution (15 M), two simulations with different system sizes were performed. Anticipating our results, we will see that finite-size effects do not appear to be significant (see Figure 1). For all calculations, cubic cells with periodic boundary conditions were employed with cell lengths determined from the experimental densities.<sup>8</sup> The production runs consisted of more than 30 ps for systems ii–iv, 10 ps for systems i and v, and 7 ps for the KOH systems.

In our simulations, the valence electronic wave functions were expanded in a plane wave basis with an energy cutoff of 70 (80) Ry for KOH (NaOH). For all atoms, the valence–core interactions were described by norm-conserving Troullier–Martins pseudopotentials.<sup>9</sup> Semicore pseudopotentials were used for both Na and K in order to deal properly with nonlinear exchange and correlation core effects.<sup>10a</sup> The gradient corrected Becke, Lee, Yang, and Parr exchange correlation functional<sup>11</sup> was employed since it has been shown to give a good description of aqueous systems.<sup>10</sup> A fictitious electronic mass<sup>5</sup> of 500 (600) au was used for KOH (NaOH), which allowed integration of the equations of motion with a time step of

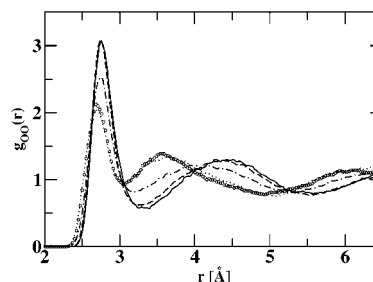


**Figure 1.** Calculated oxygen–oxygen radial distribution functions for NaOH at 0 (solid), 1.5 (dashed), 4.5 (dashed–dotted), and 15 M (dots and circles), respectively. The circles (dots) are for the larger (smaller) of the two 15 M systems. Note that the first peak decreases in amplitude and the second peak shifts dramatically with added hydroxide.

5 au (0.12 fs). All H atoms were replaced by D. The average classical energies (nuclear kinetic energy plus electronic total energy) are  $-680.621$ ,  $-904.971$ , and  $-1809.929$  au for systems ii, iv, and v, respectively.

The oxygen–oxygen radial distribution functions ( $g_{\text{OO}}$ ) (see Figure 1) display a continuous change of the water structure with the added NaOH, e.g., a significant shift of the second peak position to shorter distances. For pure water or low-concentration solutions, the second peak appears around 4.4 Å, indicating a tetrahedral short-range coordination. In contrast, at the highest concentration, 15 M, it moves to 3.68 Å. Compared to the second peak, the first peak shifts by only 0.06 Å, from 2.75 Å for pure water to 2.69 Å for the 15 M solution. However, there is a large decrease of the first peak's height. From the ratio of these two peak positions, 1.61 for pure water and 1.37 for the 15 M solution, it can be concluded that the water molecules no longer have tetrahedral coordination in the concentrated solution (a perfect tetrahedral coordination has a ratio of 1.63). This is in agreement with the structural interpretation from the NDIS experiment on a NaOH solution with a similar concentration.<sup>1</sup> The  $g_{\text{OO}}$  functions for the KOH solutions (not shown here) exhibit a similar picture, but the second peak shifts by a smaller amount. This is likely due to the fact that the smaller  $\text{Na}^+$  ion brings its neighboring water molecules closer. The shift of the first peak to shorter distances compared to pure water is mainly caused by the strong  $\text{OH}^-$  ion–water interaction.

Given a significant change of the water structure, it is expected that there would be a concomitant change of the water dynamics. To investigate the dynamical properties, we have analyzed the velocity autocorrelation power spectra of these solutions. Shown in Figure 2a are the power spectra for deuterium atoms in pure

<sup>†</sup> University of Pennsylvania.

<sup>‡</sup> Max-Planck-Institut für Festkörperforschung.

<sup>§</sup> Pohang University of Science and Technology.

<sup>⊥</sup> Centro Svizzero di Calcolo Scientifico.

<sup>||</sup> ETH Zurich.

<sup>#</sup> Present address: Dipartimento di Scienze Chimiche, Fisiche e Matematiche, Università dell'Insubria at Como, via Lucini 3, I-22100 Como, Italy.

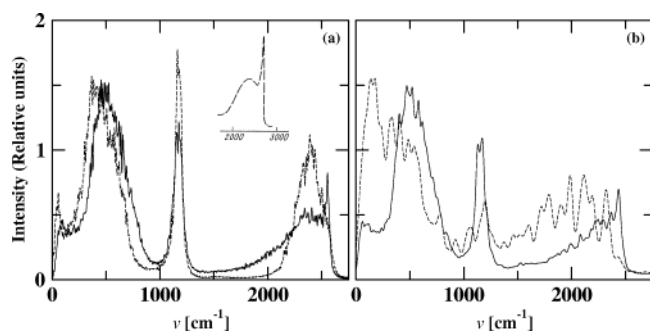


**Figure 2.** (a) Deuterium power spectrum for pure D<sub>2</sub>O (dashed line) and for 15 M NaOD solution (solid line). The experimental Raman spectrum<sup>2d</sup> is shown in the inset. (b) Deuterium power spectrum (solid line) and IR spectrum (dashed line) of 14 M KOD solution (see text).

D<sub>2</sub>O and the 15 M NaOD solution. Remarkably, the shape of the calculated spectrum for the 15 M solution resembles well the basic feature of the Raman spectrum<sup>2d</sup> at a similar concentration. (However, it should be kept in mind that the calculated power spectrum in principle contains both IR and Raman features.) Figure 2a shows that the water bending motion is essentially undisturbed by the presence of hydroxide. There is a significant broadening of the O–D stretch and a large shift of the librational band to higher frequencies. It should also be noted that the low-frequency peak moves from  $\sim 55$  cm<sup>-1</sup> for pure water to  $\sim 95$  cm<sup>-1</sup> for the 15 M solution. This agrees with the experimental low-frequency Raman spectra of pure water and hydroxide solutions.<sup>2e</sup> In addition, a spike appears at 2550 cm<sup>-1</sup> for the 15 M solution, which also shows up in the experimental Raman at 2660 cm<sup>-1</sup> and IR at 2650 cm<sup>-1</sup>.<sup>2d</sup> From an analysis of the spectrum of individual D atoms, the “free” O–D stretch of OD<sup>-</sup> is identified as being responsible for the appearance of this spike. Water molecules that are strongly hydrogen bonded to OD<sup>-</sup> are responsible for many of the other spectral features. The deuterium spectrum of the KOD system (see Figure 2b) paints a similar picture, but the spike shifts to 2440 cm<sup>-1</sup>, which could be due to the different solvation structures in these two solutions (see below). We also calculated the IR spectrum<sup>10c</sup> for the 14 M KOD solution (see Figure 2b). Interestingly, the spike due to the “free” O–D stretch is relatively IR inactive, which agrees with the experiment.<sup>2d</sup>

As mentioned above, spectroscopic experiments (IR and Raman) on concentrated solutions<sup>2</sup> suggest that a symmetric H<sub>3</sub>O<sub>2</sub><sup>-</sup> complex is the dominant solvation structure. This is, in fact, partly inferred from the IR inactivity of the free O–H stretch. However, our simulations suggest that H<sub>3</sub>O<sub>2</sub><sup>-</sup> is only a transient structure for both NaOH and KOH solutions, although it appears more frequently at higher concentrations. Repeated proton transfer, back and forth between water and OH<sup>-</sup>, is likely responsible for the reduced IR activity of the OH<sup>-</sup> stretch.

An important finding is that the solvation structure of OH<sup>-</sup> depends on the concentration. At low concentrations of NaOH or KOH, OH<sup>-</sup> prefers the H<sub>3</sub>O<sub>5</sub><sup>-</sup> structure, which was observed in a previous CPMD study<sup>6</sup> of an aqueous system with one OH<sup>-</sup> and no counterion. This structure is also consistent with the high solvation number of 5.5 for OH<sup>-</sup>, as determined from a recent dielectric relaxation experiment on a dilute NaOH solution.<sup>12</sup> (It should be noted that additional waters could coordinate with the top and bottom of the planar H<sub>3</sub>O<sub>5</sub><sup>-</sup> complex.) Although, at high concentrations, H<sub>3</sub>O<sub>5</sub><sup>-</sup> remains a stable complex, other structures are also present. For example, a planar trisolated complex, H<sub>7</sub>O<sub>4</sub><sup>-</sup>, is found to be prominent in 14 M KOH, whereas a pentasolvated complex, H<sub>11</sub>O<sub>6</sub><sup>-</sup>, is observed in 15 M NaOH. However, none of

the observed stable solvation structures has a tetrahedral geometry. This is the likely explanation of the loss of the tetrahedral short-range coordination of water in the hydroxide system, as seen in the  $g_{OO}$ . Since OH<sup>-</sup> prefers a more compact coordination shell than water, the large shift of the second peak position of the solution  $g_{OO}$  can be understood in terms of the decrease of the first-neighbor OO distance and a shift from tetrahedral to roughly octahedral coordination. However, these solvation structures differ from the tetrahedral trisolated complex found in the gas-phase ab initio calculations.<sup>4b,c</sup> This might be because these simulations were carried out in condensed phase at finite temperature while the gas-phase calculations were done for the isolated hydroxide–water clusters at 0 K. Future work is needed to investigate the influence of solvation environment and the thermal fluctuation on the stability of different solvated hydroxide complexes.

In conclusion, CPMD simulations have been carried out on a series of aqueous NaOH and KOH solutions. These calculations confirm that the structural and dynamical properties of water change significantly with the addition of hydroxide. For both the NaOH and KOH systems, the tetrahedral coordination of pure water is completely missing at high concentrations. In addition, new spectroscopic features appear, including a “free” O–H stretch, a broadening of the normal water OH stretching band, and a large blue shift of both the librational band and the low-frequency translation. Overall, these findings are in agreement with many experiments. Finally, it was demonstrated that the structural and dynamical behavior is inextricably linked to the formation of compact hydroxide–water complexes.

**Acknowledgment.** We thank Prof. Fabio Bruni for sharing experimental neutron data with us and Mark Tuckerman and Simone Rauegi for many stimulating discussions. Financial support from the National Science Foundation CHE-9623017 and a Deutscher Akademischer Austauschdienst Fellowship (J.M.P.) is gratefully acknowledged. Computer resources were provided, in part, by the Pittsburgh Supercomputing Center through NPACI.

## References

- (1) Bruni, F.; Ricci, M. A.; Soper, A. K. *J. Chem. Phys.* **2001**, *114*, 8056–8063.
- (2) (a) Busing, W. R.; Hornig, D. F. *J. Phys. Chem.* **1961**, *65*, 284–292. (b) Zatschina, P. N. *J. Struct. Chem.* **1971**, *12*, 894–898. (c) Schiöberg, D.; Zundel, G. *J. Chem. Soc., Faraday Trans. 2* **1973**, *69*, 771–781. (d) Librovich, N. B.; Maiorov, V. D. *Russian J. Phys. Chem.* **1982**, *56*, 380–383. (e) Amo, Y.; Tominaga, Y. *J. Raman Spectrosc.* **2000**, *31*, 547–553.
- (3) Agmon, N. *Chem. Phys. Lett.* **2000**, *319*, 247–252.
- (4) (a) Meot-Ner, M.; Speller, C. V. *J. Phys. Chem.* **1986**, *90*, 6616–6624. (b) Grimm, A. R.; Bacskay, G. B.; Haymet, A. D. J. *Mol. Phys.* **1995**, *86*, 369–384. (c) Novoa, J. J.; Mota, F.; del Valle, C. P.; Planas, M. *J. Phys. Chem. A* **1997**, *101*, 7842–7853.
- (5) Car, R.; Parrinello, M. *Phys. Rev. Lett.* **1985**, *55*, 2471–2474.
- (6) Tuckerman, M. E.; Laasonen, K.; Sprik, M.; Parrinello, M. *J. Chem. Phys.* **1995**, *103*, 150–161.
- (7) Hutter, J.; Alavi, A.; Deutsch, T.; Bernasconi, M.; Goedecker, S.; Marx, D.; Tuckerman, M.; Parrinello, M. *CPMD*, version 3.4; MPI für Festkörperforschung and IBM Research Laboratory: Stuttgart and Zurich, 1995–2000.
- (8) Lide, D. A. *CRC Handbook of Chemistry and Physics*; CRC Press: Boca Raton, FL, 1991.
- (9) Troullier, N.; Martins, J. L. *Phys. Rev. B* **1991**, *43*, 1993–2006.
- (10) (a) Ramanian, L. M.; Bernasconi, M.; Parrinello, M. *J. Chem. Phys.* **1999**, *111*, 1587–1591. (b) Sprik, M.; Hutter, J.; Parrinello, M. *J. Chem. Phys.* **1996**, *105*, 1142–1152. (c) Silvestrelli, P. L.; Bernasconi, M.; Parrinello, M. *Chem. Phys. Lett.* **1997**, *277*, 478–482.
- (11) (a) Becke, A. D. *Phys. Rev. A* **1988**, *38*, 3098–3100. (b) Lee, C.; Yang, W.; Parr, R. C. *Phys. Rev. B* **1988**, *37*, 785–789.
- (12) Buchner, R.; Hefter, G.; May, P. M.; Sipos, P. *J. Phys. Chem. B* **1999**, *103*, 11186–11190.

JA020350G